

## Nonexponential London Penetration Depth of FeAs-Based Superconducting $R\text{FeAsO}_{0.9}\text{F}_{0.1}$ ( $R = \text{La, Nd}$ ) Single Crystals

C. Martin, M. E. Tillman, H. Kim, M. A. Tanatar, S. K. Kim, A. Kreyssig, R. T. Gordon, M. D. Vannette, S. Nandi, V. G. Kogan, S. L. Bud'ko, P. C. Canfield, A. I. Goldman, and R. Prozorov\*

Ames Laboratory and Department of Physics & Astronomy, Iowa State University, Ames, Iowa 50011, USA  
(Received 12 March 2009; published 18 June 2009)

The superconducting penetration depth  $\lambda(T)$  has been measured in  $R\text{FeAsO}_{0.9}\text{F}_{0.1}$  ( $R = \text{La, Nd}$ ) single crystals ( $R$ -1111). In Nd-1111, we find an upturn in  $\lambda(T)$  upon cooling and attribute it to the paramagnetism of the Nd ions, similar to the case of the electron-doped cuprate Nd-Ce-Cu-O. After the correction for paramagnetism, the London penetration depth variation is found to follow a power-law behavior,  $\Delta\lambda_L(T) \propto T^2$  at low temperatures. The same  $T^2$  variation of  $\lambda(T)$  was found in nonmagnetic La-1111 crystals. Analysis of the superfluid density and of penetration depth anisotropy over the full temperature range is consistent with two-gap superconductivity. Based on this and on our previous work, we conclude that both the  $R\text{FeAsO}$  (1111) and  $\text{BaFe}_2\text{As}_2$  (122) families of pnictide superconductors exhibit unconventional two-gap superconductivity.

DOI: 10.1103/PhysRevLett.102.247002

PACS numbers: 74.25.Nf, 74.20.Mn, 74.20.Rp, 74.25.Ha

A year after the discovery of iron-pnictide superconductors [1], the order parameter (OP) symmetry still remains an important open question. The pnictides are complex superconductors with an influence from magnetism, similar to the cuprates [2], and multigap superconductivity, as in  $\text{MgB}_2$  [3]. Theory predicts that a spin-density wave instability and multiple Fermi surface (FS) sheets can give rise to a complex superconducting OP. It can have opposite signs on different sheets of the FS and have  $s$ -wave ( $s^\pm$ -wave) [4], anisotropic  $s$ -wave [5], extended  $s$ -wave with nodes [6], or  $d_{x^2-y^2}$ -wave symmetry [7].

The London penetration depth,  $\lambda_L(T)$ , is among the most useful probes of the OP symmetry [8]. A fully gapped FS leads to exponential saturation of  $\lambda_L(T \rightarrow 0)$  below the temperature determined by the minimum value of the gap. This can either be due to pairing anisotropy or/and different gap amplitudes on different sheets of the FS. The presence of the gap zeroes (point or line nodes) on the FS leads to a nonexponential variation of  $\lambda_L(T)$ , e.g., power-law behavior. In the high- $T_c$  cuprates, precision measurements of  $\lambda_L(T)$  were the first to show the existence of  $d$ -wave pairing [9]. Measurements of  $\lambda(T)$  in FeAs compounds reveal a contradictory picture. Extensive studies of both electron-doped  $\text{Ba}(\text{Fe, Co})_2\text{As}_2$  [10] and hole-doped  $(\text{Ba, K})\text{Fe}_2\text{As}_2$  [11] (122) have found  $\lambda_L(T) \propto T^2$  behavior down to  $\approx 0.02T_c$ , which may be a signature of the unconventional  $s^\pm$  state [12,13]. Microwave measurements in hole-doped 122 suggest a fully gapped state with two gaps [14], whereas  $\mu\text{SR}$  measurements show a linear temperature dependence of the superfluid density, suggesting a nodal gap [15].

Previous studies on single crystals of Sm-1111 [16], Pr-1111 [17,18], as well as in our own experiments on Nd-1111 [19], have claimed exponential behavior of  $\lambda(T)$ , consistent with a fully gapped FS. These results were supported by ARPES [20] and by point contact spectroscopy [21,22], whereas  $\mu\text{SR}$  [23] and NQR [24] results could be interpreted as both, multigap  $s$ - or  $d$ -wave state. Contrary, measurements of  $\lambda(T)$  in stoichiometric 1111  $\text{LaFePO}$  suggest the existence of line nodes [25].

In this Letter we report penetration depth measurements in  $R\text{FeAsO}_{0.9}\text{F}_{0.1}$  ( $R = \text{La, Nd}$ ) single crystals. Using samples much larger than those used in our previous study [19] as well as reported in Refs. [16,17], we have achieved a much better signal-to-noise (S/N) ratio and found that, contrary to previous observations,  $\lambda(T)$  is not exponentially flat at low temperatures. Instead, it shows an upturn due to paramagnetic contribution from the  $\text{Nd}^{3+}$  ions. Correcting the data for this paramagnetism, we have determined that the London penetration depth,  $\lambda_L(T)$  does not saturate down to  $0.02T_c$  and is best described by the power-law  $\Delta\lambda_L(T) \propto T^2$ . Furthermore, measurements on single crystals of La-1111 with nonmagnetic ion  $\text{La}^{3+}$  do not show an upturn down to  $0.06T_c$  and reveal the same power-law without any corrections. A similar situation was resolved ten years ago in the electron-doped cuprate  $\text{Nd}_{1.85}\text{Ce}_{0.15}\text{CuO}_{4-x}$  (NCCO) [26,27].

Single crystals of  $R\text{FeAsO}_{0.9}\text{F}_{0.1}$  (nominal O and F composition) were extracted from 5 mm diameter pellets synthesized under high pressure [28]. Individual crystals have dimensions up to  $650 \times 180 \times 120 \mu\text{m}^3$  for Nd-1111 and  $330 \times 240 \times 10 \mu\text{m}^3$  for La-1111 (left inset of Fig. 1). Here we present results for the largest samples with the highest S/N ratio. Similar results were obtained in four other somewhat smaller crystals. The mean  $T_c$  was 45 K for Nd-1111 and 14 K for La-1111 crystals. According to Refs. [1,29], our samples are underdoped.

The samples were characterized using synchrotron x rays (6ID-D beam line in the MUCAT sector at the Advanced Photon Source, Argonne) with an energy of 99.6 keV and an absorption length of 1.5 mm, probing

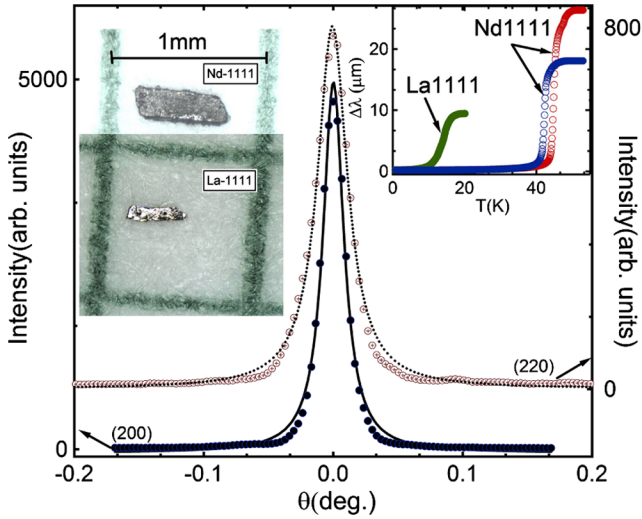


FIG. 1 (color online). Transverse scans through the (200) and (220) Bragg reflections of the Nd-1111 single crystal. The lines are fits to Lorentzians yielding a full width half maximum of  $0.019$  and  $0.028^\circ$ , respectively. Left inset: photographs of Nd-1111 (top) and La-1111 (bottom) single crystals. Right inset:  $\Delta f(T)$  in the full temperature range for three samples.

throughout the sample thickness. The incident beam was collimated to  $0.1 \times 0.1 \text{ mm}^2$  and the sample  $c$  direction was aligned parallel to the beam. Two-dimensional scattering patterns were measured in detail in Ref. [30]. Stepwise translations of the sample perpendicular to the incident beam allowed measurements of the spatially resolved diffraction patterns in the basal  $ab$ -plane. The entire sample was scanned and no impurities, misoriented grains or diffuse signals from disordered material were detected. The excellent quality of the single crystals can be seen from transverse scans, at room temperature, through selected Bragg reflections, Fig. 1. We find sharp peaks with widths of  $0.019$  and  $0.028^\circ$ , typical of high quality single crystals. The diffraction pattern did not change qualitatively on cooling down to  $15 \text{ K}$ , revealing no traces of the structural transition that is observed in the nonsuperconducting parent compound.

The magnetic penetration depth,  $\lambda(T)$ , was measured by placing the sample inside a  $1 \mu\text{H}$  inductor of a self-resonating tunnel-diode resonator (TDR) with resonant frequency  $f_0 = 1/2\pi\sqrt{LC} \approx 14 \text{ MHz}$ . The excitation ac magnetic field,  $H_{ac} \sim 10 \text{ mOe}$ , is much smaller than the lower critical field  $H_{c1} \sim 100 \text{ Oe}$ , assuring that the sample is in the Meissner state. The measured quantity is the shift in the resonant frequency,  $\Delta f \equiv f(T) - f_0 = -4\pi\chi(T)G$ , where  $\chi$  is the total magnetic susceptibility and  $G \approx f_0 V_s / 2V_c(1 - N)$  is a geometric calibration factor defined by the coil,  $V_c$ , and the sample,  $V_s$ , volumes and the demagnetization factor  $N$ .  $G$  is measured directly by pulling the sample out of the coil at the lowest temperature [8]. The susceptibility in the Meissner state can be written in terms of  $\lambda_L(T)$ ,  $\mu(T)$ , and a characteristic sample dimension  $w$  as  $4\pi\chi(T) = [\sqrt{\mu(T)}\lambda_L(T)/w] \times$

$\tanh[\sqrt{\mu}w/\lambda_L(T)] - 1$ , where  $\mu(T)$  is the normal state paramagnetic permeability [8,31].

Figure 2(a) shows the frequency shifts for Nd-1111 (main frame) and La-1111 (inset) crystals at low temperatures (the whole range is shown in the inset in Fig. 1). The samples were mounted with  $H_{ac} \parallel c$ , so that  $\Delta f \propto \Delta\lambda_{ab}$ . Note that the total frequency change over  $15 \text{ K}$  is about  $1 \text{ Hz}$ , which is less than  $0.1 \text{ ppm}$ . However, this is still significantly larger than the noise level of our system, as shown in Fig. 2(a). Whereas the data in La-1111 are monotonic, the measured  $\Delta f(T)$  in Nd-1111 shows an upturn below  $4 \text{ K}$ . A similar upturn in the electron-doped cuprate NCCO was explained by the local moment magnetism of the Nd ions [26,27]. In general, screening of a magnetic field by a paramagnetic superconductor with  $\mu > 1$  (in normal state) is described by London equation with the effective penetration depth  $\lambda(T, \mu) = \lambda_L(T)/\sqrt{\mu(T)}$ . Simultaneously, the measured frequency shift in a resonant technique is also proportional to  $\mu$ . These two effects combined give  $\Delta f(T) = G\sqrt{\mu}\lambda_L(T)$  [26,27]. If we assume Curie-Weiss behavior for the mag-

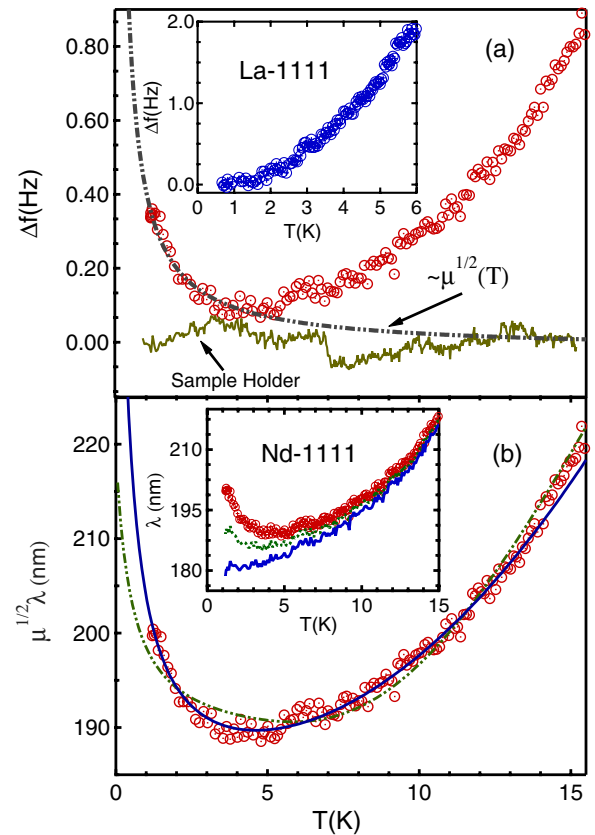


FIG. 2 (color online). (a) Frequency shift  $\Delta f(T)$  for a Nd-1111 crystal (symbols), contribution from the sample holder (continuous line) and  $\sqrt{\mu}$  (dashed line). Inset:  $\Delta f(T)$  for the La-1111 crystal. (b) Low-temperature region of  $\lambda(T)$  in the Nd-1111 crystal. The lines are fits to Eq. (1a) (dashed line) and Eq. (1b) (continuous line). Inset: Original data (symbols) and  $\lambda_L(T)$  obtained after dividing by  $\sqrt{\mu}$  from a fit to Eq. (1a) (dots) and to Eq. (1b) (continuous line).

netic susceptibility,  $\chi(T) = C/(T + \theta)$ , with  $C$  being the Curie constant ( $4\pi$  factor included) and  $\theta$  being the Curie-Weiss temperature, we obtain an upturn in  $\Delta f(T)$  provided the paramagnetic increase is larger than the decrease due to  $\lambda_L(T)$ . Figure 2(a) shows that  $\sqrt{\mu(T)}$  clearly dominates the experimental data below 4 K. To subtract the contribution of the paramagnetic term, we fit the data assuming  $\lambda_L(T)$  to be either exponential, Eq. (1a), or power law, Eq. (1b). Special care was taken to fit only in the temperature range in which the total variation of the penetration depth did not exceed 5%, i.e., where the temperature dependence of the gap can be neglected.

$$\lambda(T) = \sqrt{\mu(T)}\lambda(0)\left[1 + \sqrt{\frac{\pi\Delta_0}{2T}}\exp\left(-\frac{\Delta_0}{T}\right)\right], \quad (1a)$$

$$\lambda(T) = \sqrt{\mu(T)}\lambda(0)[1 + AT^n]. \quad (1b)$$

As shown in Fig. 2(b), for both forms the best fits are obtained for  $\theta \approx 0.2$  K, which suggests the possibility of antiferromagnetic order of the Nd moments. A fit to the  $s$ -wave BCS form Eq. (1a) with  $\Delta_0$  and the Curie-Weiss constant  $C$  as the free parameters yields  $\Delta_0 = (0.8 \pm 0.2)T_c$  and  $C = 0.085 \pm 0.03$ . The best fit of the data to the power law, Eq. (1b), is obtained for  $n = 2.1 \pm 0.2$ . This function not only reproduces the data accurately, but gives a narrow range of the variation for  $C = 0.18 \pm 0.02$  in between  $C = 0.1$  obtained from the neutron diffraction [32] and  $C = 0.5$  for the free  $\text{Nd}^{3+}$  ion. The inset of Fig. 2(b) shows the London penetration depth  $\lambda_L(T)$  obtained after dividing by  $\sqrt{\mu(T)}$  for two sets of values ( $C, \theta$ ): (0.085, 0.2) from the best fit to Eq. (1a) and (0.18, 0.2) from the best fit to Eq. (1b). We notice that an assumption of exponential  $\lambda_L(T)$  does not remove the low-temperature upturn. It may be argued that the fit to Eq. (1b) is better because of an additional fitting parameter. To check if this is the case, we tried a generalized exponential BCS expression, leaving the prefactor of the exponential as a free parameter in Eq. (1a). Indeed, it improves the quality of the fit, particularly in the high temperature region. However, statistical analysis of the residuals shows that this fit is still inferior compared to the power law.  $\lambda_L(T)$  obtained from the fit to Eq. (1b) does not saturate exponentially for  $T \leq 6$  K, contrary to earlier reports that analyzed the *total* measured  $\lambda(T)$  [16,17,19]. As shown in Fig. 3,  $\lambda_L(T) \sim T^2$  down to  $0.02T_c$  for all studied  $R$ -1111 crystals. This remarkable finding together with the results from Ref. [10,11], suggest that the nearly quadratic temperature dependence of the London penetration depth is a universal characteristic of the iron-pnictide superconductors.

In addition to unconventional power-law behavior of  $\lambda(T)$ , we show below that the penetration depth anisotropy and superfluid density are consistent with the existence of two gaps in  $R$ -1111. To calculate the anisotropy  $\gamma_\lambda(T) = \lambda_c/\lambda_{ab}$  (both quantities are now London penetration depths after accounting for the paramagnetic contribution), we

need to know the absolute values of  $\lambda_{ab}(T)$  and  $\lambda_c(T)$ . For the in-plane penetration depth,  $\mu\text{SR}$  experiments give  $\lambda_{ab}(0) = 200$  nm [33]. To obtain the absolute value for  $\lambda_c(T)$ , we use the anisotropy of  $H_{c2}(T)$  near  $T_c$  as described in Ref. [34]. From our TDR measurements [19] as well as from resistivity [35] and specific heat [36] measurements,  $\gamma_\lambda = \gamma_\xi(T \leq T_c) \approx 4-5$  at  $T_c$ . The inset of Fig. 4 shows  $\gamma_\lambda(T)$  calculated assuming  $\gamma_\lambda(T_c) = 4.5$ . Regardless of the initial value chosen,  $\gamma_\lambda(T)$  increases upon cooling, reaching  $\gamma_\lambda(0) \approx 17 \pm 3$  at  $T = 0$ . Such behavior of the anisotropy was first reported in Sm- and Nd-1111 and interpreted in terms of multiband superconductivity in Ref. [37]. A similar temperature dependence was also observed in the FeAs-122 superconductors [38]. A possible explanation for the increase of  $\gamma_\lambda(T)$  upon cooling is the existence of two superconducting gaps with different magnitudes on the FS with different anisotropies [11,37,39].

Figure 4 shows the in-plane superfluid density,  $\rho(T) = \lambda^2(0)/\lambda^2(T)$ . Because of uncertainty in  $\lambda(0)$  we have used the two values of 200 nm and 350 nm that agree with the literature for the 1111 pnictides [23,33]. Inspection of  $\rho(T)$  in the full temperature range reveals a pronounced positive curvature, similar to  $\text{MgB}_2$  [40]. This prompts to try a simple  $s$ -wave two-gap model, despite the fact that the low-temperature behavior of  $\lambda_L(T)$  is clearly nonexponential. In this approach we fit the data to  $\rho(T) = \varepsilon\rho_1(\Delta_1) + (1 - \varepsilon)\rho_2(\Delta_2)$  with two clean  $s$ -wave gaps  $\Delta_1(T)$  and  $\Delta_2(T)$  along with relative densities of states,  $\varepsilon$  and  $(1 - \varepsilon)$ . Successful fits were obtained in all cases with the following values of ( $\Delta_1/k_B, \Delta_2/k_B$  and  $\varepsilon$ ): La-1111 (11.29 K, 4.16 K, 0.83) for  $\lambda(0) = 200$  nm and (14.98 K, 5.24 K, 0.82) for  $\lambda(0) = 350$  nm. For Nd-1111, we obtain (47.25 K, 14.71 K, 0.86) and (64.15 K, 21.61 K, 0.85). In all samples, the ratio between the gaps is  $\Delta_1/\Delta_2 \approx 3$ , with the

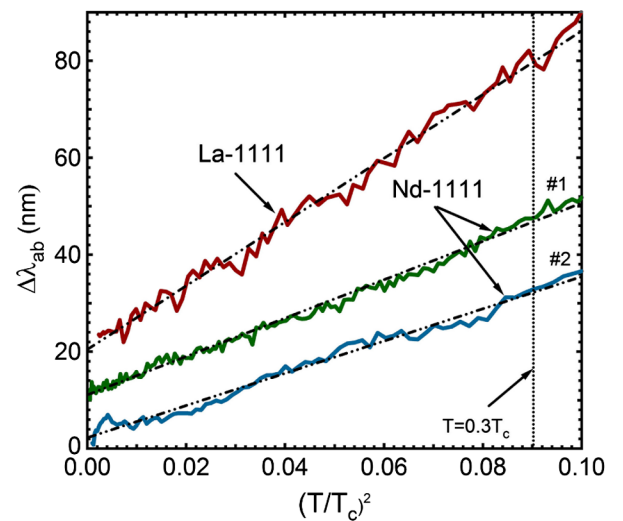


FIG. 3 (color online).  $\Delta\lambda_L$  vs  $(T/T_c)^2$  after dividing the paramagnetic contribution for two Nd-1111 samples and raw data for a La-1111 crystal (continuous lines). The curves have been shifted vertically for clarity.

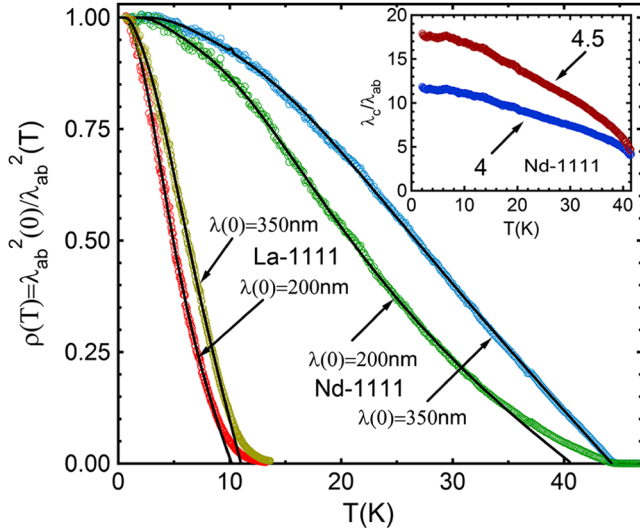


FIG. 4 (color online). The superfluid density,  $\rho(T)$ , for  $R$ -1111 crystals calculated with the two values of 200 and 350 nm for  $\lambda_L(0) =$  (symbols). Solid lines are fits to the two-gap model described in the text. Inset: temperature dependent anisotropy of the penetration depth.

large gap at the FS sheet with 80% of the total density of states. This result is similar to previous reports on Sm-1111 [16] and Pr-1111 [17,18,41]. This analysis poses two interesting questions. First, for all cases, we obtain  $\Delta_1/k_B T_c$  and  $\Delta_2/k_B T_c$  smaller than the weak-coupling limit of 1.76. These values for the gaps should result in lower  $T_c$  than experimentally observed, unless strong interband coupling is considered. In this case though, the model is not applicable any more.

Second, for the experimentally determined value of  $\lambda_{ab}(0) = 200$  nm, the superfluid density shows a strong suppression near  $T_c$ . In the vicinity of  $T_c$ , the superfluid density should be linear with temperature,  $\rho(T) = \eta(1 - T/T_c)$ . For a clean  $s$ -wave superconductor  $\eta = 2$ , whereas for  $R\text{FeAsO}_{0.9}\text{F}_{0.1}$  we obtain  $\eta \approx 1$ . This reduced slope agrees qualitatively with the theoretical calculations for the case of two  $s$ -wave gaps [42] and/or extended  $s^+$  symmetry [13] when a large interband scattering rate  $\tau_{12}$  is considered,  $\eta \propto 1/\tau_{12}$ , therefore a higher  $\tau_{12}$  will lower the slope of  $\rho(T)$  at  $T_c$ . Again, the model used for fitting in Fig. 4 does not account for possible interband scattering.

In conclusion, we find that the in-plane London penetration depth in single crystals of  $R\text{FeAsO}_{0.9}\text{F}_{0.1}$  ( $R = \text{La}, \text{Nd}$ ) follows a power-law temperature dependence,  $\Delta\lambda_{ab}(T) \propto T^2$  for  $T < T_c/3$ . The penetration depth anisotropy  $\gamma_\lambda$  increases upon cooling and combined with the behavior of  $\rho(T)$  at elevated temperatures, provides strong evidence for multigap superconductivity. The analysis of  $\rho(T)$  shows the failure of simple two  $s$ -wave gaps model used for  $\text{MgB}_2$ . Given our results on 122 family [10,11], we conclude that iron-based pnictides are unconventional multigap superconductors.

We thank D. S. Robinson for help with the x-ray experiment, A. Carrington, A. V. Chubukov, R. W. Giannetta,

I. I. Mazin, G. D. Samolyuk, J. Schmalian, and A. B. Vorontsov for discussions. Work at the Ames Laboratory was supported by the Department of Energy-Basic Energy Sciences under Contract No. DE-AC02-07CH11358. R. P. acknowledges support from the Alfred P. Sloan Foundation.

\*Corresponding author.

prozorov@ameslab.gov

- [1] Y. Kamihara *et al.*, J. Am. Chem. Soc. **130**, 3296 (2008).
- [2] J. Zhao *et al.*, Nature Mater. **7**, 953 (2008).
- [3] I. I. Mazin *et al.*, Physica (Amsterdam) **385C**, 49 (2003).
- [4] I. I. Mazin *et al.*, Phys. Rev. Lett. **101**, 057003 (2008).
- [5] R. Sknepnek *et al.*, Phys. Rev. B **79**, 054511 (2009).
- [6] S. Graser *et al.*, New J. Phys. **11**, 025016 (2009).
- [7] K. Seo *et al.*, Phys. Rev. Lett. **101**, 206404 (2008).
- [8] R. Prozorov and R. W. Giannetta, Supercond. Sci. Technol. **19**, R41 (2006).
- [9] W. N. Hardy *et al.*, Phys. Rev. Lett. **70**, 3999 (1993).
- [10] R. T. Gordon *et al.*, Phys. Rev. Lett. **102**, 127004 (2009); Phys. Rev. B **79**, 100506(R) (2009).
- [11] C. Martin *et al.*, arXiv:0902.1804.
- [12] M. M. Parish *et al.*, Phys. Rev. B **78**, 144514 (2008).
- [13] A. B. Vorontsov *et al.*, Phys. Rev. B **79**, 140507(R) (2009).
- [14] K. Hashimoto *et al.*, Phys. Rev. Lett. **102**, 207001 (2009).
- [15] T. Goko *et al.*, arXiv:0808.1425.
- [16] L. Malone *et al.*, Phys. Rev. B **79**, 140501(R) (2009).
- [17] K. Hashimoto *et al.*, Phys. Rev. Lett. **102**, 017002 (2009).
- [18] R. Okazaki *et al.*, Phys. Rev. B **79**, 064520 (2009).
- [19] C. Martin *et al.*, arXiv:0807.0876.
- [20] T. Kondo *et al.*, Phys. Rev. Lett. **101**, 147003 (2008).
- [21] T. Y. Chen *et al.*, Nature (London) **453**, 1224 (2008).
- [22] P. Samuely *et al.*, Supercond. Sci. Technol. **22**, 014003 (2009).
- [23] H. Luetkens *et al.*, Phys. Rev. Lett. **101**, 097009 (2008).
- [24] S. Kawasaki *et al.*, Phys. Rev. B **78**, 220506(R) (2008).
- [25] J. D. Fletcher *et al.*, Phys. Rev. Lett. **102**, 147001 (2009).
- [26] J. R. Cooper, Phys. Rev. B **54**, R3753 (1996).
- [27] J. D. Kokoales *et al.*, Phys. Rev. Lett. **85**, 3696 (2000); R. Prozorov *et al.*, Phys. Rev. Lett. **85**, 3700 (2000).
- [28] R. Prozorov *et al.*, New J. Phys. **11**, 035004 (2009).
- [29] L. Fang *et al.*, J. Cryst. Growth **311**, 358 (2009).
- [30] A. Kreyssig *et al.*, Phys. Rev. B **76**, 054421 (2007).
- [31] R. Prozorov *et al.*, Phys. Rev. B **62**, 115 (2000).
- [32] Y. Qiu *et al.*, Phys. Rev. Lett. **101**, 257002 (2008).
- [33] R. Khasanov *et al.*, Phys. Rev. B **78**, 092506 (2008).
- [34] M. A. Tanatar *et al.*, Phys. Rev. B **79**, 094507 (2009).
- [35] Y. Jia *et al.*, Appl. Phys. Lett. **93**, 032503 (2008).
- [36] U. Welp *et al.*, Phys. Rev. B **78**, 140510(R) (2008).
- [37] S. Weyeneth *et al.*, J. Supercond. Novel Magnetism **22**, 325 (2009); **22**, 347 (2009).
- [38] R. Prozorov *et al.*, arXiv:0901.3698; Physica (Amsterdam) **469C**, 582 (2009).
- [39] V. G. Kogan, Phys. Rev. B **66**, 020509(R) (2002); P. Miranovic *et al.*, J. Phys. Soc. Jpn. **72**, 221 (2003).
- [40] J. D. Fletcher *et al.*, Phys. Rev. Lett. **95**, 097005 (2005).
- [41] K. Matano *et al.*, Europhys. Lett. **83**, 57001 (2008).
- [42] E. J. Nicol *et al.*, Phys. Rev. B **71**, 054501 (2005).